The Journal of Immunology

Chronic Hyperglycemia Predisposes to Exaggerated Inflammatory Response and Leukocyte Dysfunction in Akita Mice

Robert Gyurko, Camille C. Siqueira, Nathaniel Caldon, Li Gao, Alpdogan Kantarci and Thomas E. Van Dyke

J Immunol 2006; 177:7250-7256; ;
doi: 10.4049/jimmunol.177.10.7250
http://www.jimmunol.org/content/177/10/7250

The Journal of Immunology is published twice each month by
The American Association of Immunologists, Inc.,
1451 Rockville Pike, Suite 650, Rockville, MD 20852

Print ISSN: 0022-1767 Online ISSN: 1550-6606.

Chronic Hyperglycemia Predisposes to Exaggerated Inflammatory Response and Leukocyte Dysfunction in Akita Mice[1]

Robert Gyurko,[2] Camille C. Siqueira, Nathaniel Caldon, Li Gao, Alpdogan Kantarci, and Thomas E. Van Dyke

The role of polymorphonuclear neutrophils (PMN) in mediating diabetic tissue damage to the periodontium was investigated in a novel model of chronic hyperglycemia, the Akita mouse. Induction of acute peritoneal inflammation in wild-type (WT) and Akita mice resulted in exaggerated IL-6 response in Akita mice (2.9-fold increase over WT values) and a markedly increased chemokine response (KC, 2.6-fold; MCP-1, 2.6-fold; and MIP-1α, 4.4-fold increase over WT values). Chemotaxis to both fMLP and WKYMVm was significantly reduced in isolated Akita PMN compared with WT PMN as measured in a Boyden chamber. Superoxide release in contrast was significantly increased in Akita PMN as measured with cytochrome *c* reduction. Bone marrow-derived Akita PMN showed partial translocation of $p47^{phox}$ to the cell membrane without external stimulation, suggesting premature assembly of the superoxide-producing NADPH oxidase in hyperglycemia. In vivo studies revealed that ligature-induced periodontal bone loss is significantly greater in Akita mice compared with WT. Moreover, intravital microscopy of gingival vessels showed that leukocyte rolling and attachment to the vascular endothelium is enhanced in periodontal vessels of Akita mice. These results indicate that chronic hyperglycemia predisposes to exaggerated inflammatory response and primes leukocytes for marginalization and superoxide production but not for transmigration. Thus, leukocyte defects in hyperglycemia may contribute to periodontal tissue damage by impairing the innate immune response to periodontal pathogens as well as by increasing free radical load in the gingival microvasculature. *The Journal of Immunology,* **2006, 177: 7250–7256.**

Diet and insulin therapy effectively prolong the life of diabetic patients, but long-term complications of high blood glucose such as cardiovascular disease, retinopathy, kidney failure, neuropathy, impaired wound healing, and periodontal disease are affecting a rapidly increasing population of patients (1). Microvascular damage is thought to be a key early event in the development of many diabetic complications, but the immediate cellular and molecular targets of chronic high blood glucose are not clearly identified. Effects of hyperglycemia on the vascular endothelium have long been suspected to cause diabetic tissue damage, since endothelial cells take up glucose passively in an insulin-independent manner (2). At least four intracellular pathways are activated by hyperglycemia in endothelial cells, including increase of polyol pathway flux, production of advanced end glycation (AGE)[3] products, activation of protein kinase C, and elevation of hexosamine flux (3). Hyperglycemia also increases superoxide production by the mitochondrial electron transport chain in endothelial cells (4). Normalizing mitochondrial superoxide levels prevents activation of the polyol pathway as well as production of AGE and activation of protein kinase C, indicating a central role for superoxide in mediating diabetic tissue damage (3, 4).

Recently, proinflammatory effects of glucose and anti-inflammatory effects of insulin have been discovered (5, 6). Levels of acute phase proteins such as IL-6 and C-reactive protein were found elevated in serum samples of diabetic women (7). Acute glucose challenge was shown to stimulate free radical release from leukocytes (8) and adipocytes (9), as well as matrix metalloproteinase 2 secretion by mononuclear cells (10). Insulin, on the other hand, decreases levels of C-reactive protein (11) and inducible NO synthase (12), and was found to be beneficial in acutely ill patients regardless of blood glucose levels (5).

The incidence and severity of periodontal disease is increased in diabetes patients (13, 14). Hyperglycemia plays an important role because both insulin-dependent and non-insulin-dependent diabetes patients are affected, and HbA1c levels inversely correlate with periodontal health (14). Several aspects of diabetic damage to the periodontium have been explored, such as the role of AGE (15), T cell activation (16), and polymorphonuclear neutrophil (PMN)-mediated free radical damage (14). PMN are of particular interest because both acute and chronic PMN deficiency (neutropenia) cause severe oral ulcers and periodontal disease, indicating that PMN are essential in oral mucosal defense (17, 18). However, the role of PMN is controversial as activated PMN has been shown to contribute to host tissue damage in periodontal disease as well as in other conditions such as pyelonephritis, ischemia-reperfusion injury, rheumatoid arthritis, and cystic fibrosis (19–21). In this article, we use a novel genetic model of chronic hyperglycemia, the Akita mouse, to explore PMN function in chronic hyperglycemia and its potential impact on periodontal tissue damage.

Akita mice carry a naturally occurring point mutation in the *Ins2* insulin gene, rendering β cells incapable of insulin secretion in a

Department of Periodontology and Oral Biology, Boston University, Boston, MA 02118

Received for publication April 7, 2006. Accepted for publication September 4, 2006.

The costs of publication of this article were defrayed in part by the payment of page charges. This article must therefore be hereby marked *advertisement* in accordance with 18 U.S.C. Section 1734 solely to indicate this fact.

[1] This work was supported by U.S. Public Health Service Grants DE14568, DE16933, and DE15566.

[2] Address correspondence and reprint requests to Dr. Robert Gyurko, 100 East Newton Street, Suite 107, Boston, MA 02118. E-mail address: gyurko@bu.edu

[3] Abbreviations used in this paper: AGE, advanced end glycation; PMN, polymorphonuclear neutrophil; WT, wild type; BM, bone marrow; CEJ-ABC, cementoenamel junction and alveolar bone crest distance.

0022-1767/06/$02.00

dominant negative fashion (22–24). Akita mice are characterized by hyperglycemia, polydipsia, and polyuria, but no obesity, infertility, or immunological alterations have been described to date. Histological signs of glomerulosclerosis have been described in 20-wk-old Akita mice and renal function impairment after age 30 wk (25). Evidence of elevated oxidative stress was also found in the kidney of Akita mice in the form of N^{ε}-(hexanonyl)lysine and dityrosine, two markers of lipid peroxide-derived protein covalent modification (26).

Materials and Methods

Mice

Heterozygous $Ins2^{Akita}$ (Akita) and wild-type (WT) C57BL/6 mice of both sexes were purchased from The Jackson Laboratory. Adult mice (age 8–14 wk) of both sexes were used in experiments. Mean body weights were: WT, 23.3 ± 2.4 g; Akita, 21.8 ± 2.7 g ($p = 0.2$). All mouse experiments were in conformity with the standards of the Public Health Service Policy on Humane Care and Use of Laboratory Animals and were approved by the Institutional Animal Care and Use Committee of Boston University. Mice were fed standard laboratory chow and water ad libitum. Blood glucose was measured at sacrifice from the femoral vein blood of all experimental animals using a digital glucometer (Accu-Chek Advantage).

Abdominal lavage fluid collection

Mice were injected i.p. with 1 ml of zymosan A solution (1 mg/ml in PBS; Sigma-Aldrich). Mice were sacrificed 2 h (for cytokine measurements) or 12–14 h (for leukocyte collection) after zymosan injection. At the time of sacrifice, the abdominal skin was retracted to expose the abdominal muscles. Using a 22-gauge needle, 5 ml of sterile PBS was injected into the peritoneal cavity and then withdrawn to collect abdominal lavage fluid.

Cytokine measurements

Cytokines and chemokines were measured simultaneously using a multiplex bead immunoassay (Mouse Cytokine 20-plex; BioSource International). Abdominal lavage fluid was collected 2 h after zymosan injection. The cellular content of the lavage fluid was removed by centrifugation and the supernatant was assayed with the multiplex bead immunoassay. Cytokine concentrations (picograms per milliliter) measured in the lavage fluid sample were multiplied with the injected lavage fluid volume (5 ml) and reported as picograms per mouse.

PMN isolation by gradient density centrifugation

Abdominal lavage fluid collected 12–14 h after zymosan injection was layered on top of a discontinuous gradient of Histopaque 1119 and Histopaque 1083 (Sigma-Aldrich) and centrifuged at 700 × *g* for 30 min. PMN were removed from the interface of 1119 and 1083 layers, washed in 10 ml of PBS, and resuspended in 1 ml in PBS containing 0.1% BSA. Cell viability was similar in WT and Akita samples (95%) as assessed by trypan blue dye exclusion assay. Average neutrophil content of the 1119/1083 interface cell layer was 76% as assessed with differential cell count using Wright-Giemsa stain (Accustain; Sigma-Aldrich).

Leukocyte chemotaxis

A Boyden chamber fitted with a cellulose nitrate membrane (5-μm pore size) was used for chemotaxis experiments. Leukocytes were collected by abdominal lavage 12–14 h after zymosan injection and PMN were isolated by density gradient centrifugation as described above. fMLP (10 nM; Sigma-Aldrich) or WKYMVm (1 nM; AnaSpec) resuspended in Gey's balanced salt solution (Sigma-Aldrich) was added in the lower chamber and 10^6 PMN were incubated in the upper chamber at 37°C in 5% CO_2 for 2 h. After incubation, filters were fixed with methanol and stained with hematoxylin. Cells that migrated to the basal side of the membrane were counted under a microscope and expressed as cells per square millimeter membrane surface.

Superoxide measurement

Superoxide release was measured by colorimetric determination of superoxide dismutase-inhibitable cytochrome *c* reduction. Leukocytes were collected by abdominal lavage 12–14 h after zymosan injection and PMN were isolated by density gradient centrifugation as described above. PMN (5×10^5) were incubated in 200 μl of Gey's balanced salt solution in the presence or absence of 1 μM fMLP. The cell suspension was maintained at 37°C during superoxide assessment. Reduction of cytochrome *c* (0.3 mg/ml; Sigma-Aldrich) was monitored by measuring light absorbance at 550 nm with a SpectraMax 340 microplate reader for 5 min in the presence or absence of superoxide dismutase. Maximum velocity was calculated using SoftMax Pro, version 4.3 (Molecular Devices).

Acute hyperglycemic challenge of isolated PMN

PMN were isolated from abdominal lavage fluid of WT mice as described above. PMN were resuspended at 10^7 cells/ml in RPMI 1640 (Invitrogen Life Technologies) containing 5.5 or 25 mM glucose. PMN were incubated in a tissue culture incubator at 37°C in 5% CO_2 for 3 h. At the end of the incubation period, cells were pelleted by centrifugation, resuspended in PBS, and assessed for chemotaxis or superoxide release as described above.

Bone marrow (BM) neutrophil isolation

Mice were sacrificed by CO_2 asphyxiation and the femur and the tibia were removed. The epiphysis was removed from both ends of the bones and the marrow was flushed out with 5 ml of PBS containing BSA (0.1%) using a syringe and a 25-gauge needle. Cells were dissociated by pipetting, pelleted by centrifugation at 400 × *g* for 10 min at 4°C, and resuspended in PBS containing 0.1% BSA. PMN were isolated from BM cell suspension by gradient density centrifugation as described above. Average PMN content of the 1119/1083 interface cell layer was 81%.

Subcellular fractionation

BM PMN were resuspended in 400 μl of extraction buffer (50 mM Tris-HCl, 50 mM 2-ME, 10 mM EGTA, 5 mM EDTA, 1 mM PMSF, and 10 mM benzamidine (pH 7.5)) containing Complete Proteinase Inhibitor Cocktail (Roche) and sonicated at 15 W for 15 s on ice. The cell lysate was centrifuged at 100,000 × *g* for 60 min at 4°C. The supernatant containing the cytosolic fraction was frozen at −80°C until analysis. The pellet containing the membrane fraction was extracted again in the same fashion with the addition of 0.5% Triton X-100 to the extraction buffer to obtain the membrane-associated protein fraction. Protein concentration was measured with the Bradford protein assay (Bio-Rad).

Western blotting

Cytosolic and membrane-associated protein samples were boiled in Laemmli sample buffer, loaded on 10% SDS-polyacrylamide gel (80 μg protein/lane), and electrophoresed at 90 V for 2 h. Proteins were transferred to a polyvinylidene difluoride membrane and incubated with $p47^{phox}$ Ab (1/1000 dilution; Upstate Biotechnology) or $gp91^{phox}$ Ab (1/500 dilution; Upstate Biotechnology) in PBS containing 1% milk. Membranes were washed and incubated with goat anti-rabbit secondary Ab (1/2000 dilution; Cell Signaling Technology) for 1 h at room temperature. Protein bands were visualized with luminol-enhanced chemiluminescence detection reagent (Cell Signaling Technology) followed by autoradiography.

Intravital microscopy

Mice were anesthetized i.p. with a mixture of ketamine (100 mg/kg body weight) and xylazine (5 mg/kg). FITC-dextran (6 mg/kg; Sigma-Aldrich) and rhodamine 6G (0.15 mg/kg; Molecular Probes) were injected through a tail vein to label the microvasculature and leukocytes, respectively (27). To expose gingival vessels, the lower lip was retracted with a 5-0 silk ligature and the gingiva adjacent to the lower central incisors was positioned against a glass plate placed over the objective of an inverted fluorescent microscope (Zeiss). The exposed gingiva was submerged in prewarmed bicarbonate buffer (pH 7.4). Body temperature was held between 36 and 37°C using a rectal thermometer, a temperature controller (DigiSense; Eutech Instruments), and a heating pad. To induce gingival inflammation, mice were injected intragingivally with TNF-α (100 ng in 10 μl) or PBS as control under rapid isoflurane (2%) inhalation anesthesia 2 h before the experiment. Gingival vessels and circulating leukocytes were observed with a ×40 LD (Zeiss) objective. Thirty-second-long video images were captured using a microscope-mounted video camera (Sony DFW-X700; Sony) and stored directly on a computer hard disk.

Ligature-induced alveolar bone loss

Mice were anesthetized i.p. with a mixture of ketamine (100 mg/kg) and xylazine (5 mg/kg). A 9-0 silk suture was placed into the gingival sulcus of the upper left second molar and tied around the tooth. Three weeks later, mice were sacrificed; the maxilla was cleaned and stained with methylene blue (1% in water). The distance between the cementoenamel junction and the alveolar bone crest (CEJ-ABC distance) was determined as a measurement of alveolar bone loss (28).

Statistical analysis

Comparisons between WT and Akita measurements were analyzed using the nonpaired two-tailed Student's *t* test. All data are expressed as mean ± SD.

Results

Exaggerated cytokine release in Akita mice during zymosan-induced acute peritoneal inflammation

Blood glucose measurements were routinely performed at sacrifice of experimental animals. Blood glucose was markedly higher in Akita mice (25.8 ± 9.4 mM) compared with WT mice (10.9 ± 4.4 mM, $p < 0.001$, $n = 28$ each group). The inflammatory response in Akita mice was first assessed by inducing acute peritoneal inflammation with i.p. injection of zymosan (1 mg in 1 ml of PBS). Levels of 20 inflammatory cytokines were measured simultaneously using a multiplex bead immunoassay in abdominal lavage fluid 2 h after zymosan injection and were compared with cytokine levels detected in mice without zymosan injection. Eleven of the 20 cytokines were above detection levels in the 5 ml of abdominal lavage fluid 2 h after zymosan injection (Table I). In unstimulated mice, two chemokines, MCP-1 and MIP-1α, were at moderately but significantly lower levels in Akita mice compared with WT mice. Zymosan injection in contrast elicited markedly exaggerated response in four cytokines in Akita mice. Among the classical proinflammatory cytokines IL-6 levels were significantly higher in Akita mice compared with WT mice, whereas IL-1β, GM-CSF, and IFN-γ remained unchanged. Mean TNF-α levels were slightly but not significantly higher in Akita mice with or without zymosan. Moreover, three of the five chemokines tested were markedly higher in zymosan-injected Akita mice compared with similarly treated WT mice, including the mouse IL-8 analog KC, as well as MCP-1 and MIP-1α (Table I). No significant differences were found in plasma cytokine levels of unstimulated WT and Akita mice (data not shown). Leukocyte accumulation in the peritoneum was also detected 2 h after zymosan injection in both strains with similar yields (WT, $6.0 \times 10^6 \pm 2.0 \times 10^6$ leukocyte/mouse; Akita, $5.7 \times 10^6 \pm 2.2 \times 10^6$ leukocyte/mouse, $p = 0.8$, $n = 5–6$) containing primarily PMN (WT, 87 ± 3%; Akita, 89 ± 6%) as well as lymphocytes (WT, 7 ± 2%; Akita, 6 ± 3%) and monocytes (WT, 6 ± 1%; Akita, 4 ± 2%). Abdominal lavage fluid from unstimulated WT and Akita mice yielded no PMN.

Chronic hyperglycemia impairs leukocyte chemotaxis in vivo and in vitro

PMN were collected from abdominal lavage fluid 12–14 h after zymosan injection, representing the time point for maximum PMN recruitment (29). The differential cell count in abdominal lavage fluid at 12–14 h poststimulation was similar between WT and Akita mice (lymphocytes, WT: 66 ± 9%; Akita: 72 ± 10%; monocytes WT: 11 ± 5%; Akita: 11 ± 4%; PMN: WT: 23 ± 7%; Akita: 17 ± 10%). Total cell yields in contrast were significantly lower in Akita mice (WT, $24.4 \times 10^6 \pm 6.3 \times 10^6$ leukocyte/mouse; Akita, $13.2 \times 10^6 \pm 8.4 \times 10^6$ leukocyte/mouse, $p = 0.04$, $n = 9$ mice each group). To assess PMN chemotaxis in vitro, PMN were incubated in a Boyden chamber in the presence or absence of chemotactic agents fMLP (10 nM) or WKYMVm (1 nM) for 2 h. Cells that had migrated through the cellulose nitrate membrane were stained with hematoxylin and counted. There was no difference in unstimulated (random) cell migration between WT and Akita PMN (WT, 3.1 ± 1.7 cells/mm^2; Akita,: 2.9 ± 0.8 cells/mm^2, $p = 0.87$, $n = 6$ mice each group). Agonist-specific chemotaxis was expressed as the difference between stimulated and unstimulated cell migration. fMLP induced chemotaxis in both WT and Akita PMN ($p < 0.01$). However, significantly fewer Akita

Table I. *Cytokine levels in peritoneal fluid at baseline and after zymosan injection*[a]

	TNF-α	IL-1β	IL-6	GM-CSF	IFN-γ	IL-10	KC	MCP-1	MIG	MIP-1α	IP-10
WT	2 ± 3	170 ± 1	nd	32 ± 7	nd	828 ± 835	35 ± 61	109 ± 2	nd	179 ± 5	891 ± 62
Akita	6 ± 10	167 ± 2	nd	34 ± 47	nd	1197 ± 2073	51 ± 87	99 ± 5[b]	nd	125 ± 31[b]	819 ± 51
WT + zymosan	139 ± 94[c]	89 ± 64	2180 ± 1744	42 ± 40	7 ± 1	5492 ± 2730[c]	1483 ± 1260	617 ± 620	37 ± 9	266 ± 224	400 ± 269[c]
Akita + zymosan	203 ± 96[d]	81 ± 61	6290 ± 1902[e]	34 ± 31	7 ± 1	5150 ± 4187	3888 ± 1194[d,e]	1577 ± 593[d,e]	40 ± 10	1174 ± 737[d,e]	384 ± 187[d]

[a] Peritoneal lavage fluid from unstimulated and zymosan-injected (1 mg/ml) WT and Akita mice. Cytokines were measured with a multiplex bead immunoassay. The following cytokines were also assayed but were below assay detection limits: fibroblast growth factor; IL-1α, IL-2, IL-4, IL-5, IL-12, IL-13, IL-17, and VEGF. Values shown are mean ± SD of cytokine amounts in picograms per mouse ($n = 5–6$ mice each group). Statistically significant differences ($p < 0.05$) are shown as follows: [b] between WT and Akita, [c] between WT and WT + zymosan, [d] between Akita and Akita + zymosan, and [e] between WT + zymosan and Akita + zymosan (nd, not detected). MIG, Monokine induced by IFN-γ; IP-10, IFN-inducible protein 10.

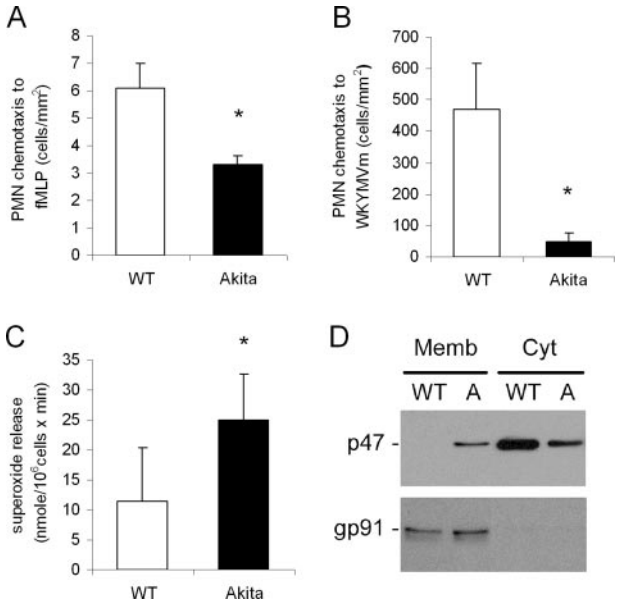

FIGURE 1. Leukocyte dysfunction in hyperglycemia. *A,* PMN migration across a cellulose-nitrate membrane in a Boyden chamber in response to fMLP. Zymosan-elicited PMN from WT and Akita mice were incubated with 10 nM fMLP or PBS for 2 h. fMLP-induced migration is expressed as the difference between fMLP-stimulated and unstimulated cell migration in PBS ($p = 0.011$, $n = 6$ mice each group). *B,* The effect of the synthetic chemotactic peptide WKYMVm (1 nM) on zymosan-elicited PMN in a Boyden chamber ($p = 0.008$, $n = 4$ mice each group). *C,* Superoxide release from WT and Akita PMN upon fMLP stimulation. Zymosan-elicited peritoneal PMN were incubated with fMLP (1 μM) or PBS for 5 min. Superoxide release was measured as the superoxide dismutase-inhibitable reduction of cytochrome *c* and expressed as the difference between fMLP-elicited and unstimulated superoxide release in PBS ($p = 0.018$, $n = 6$ mice each group). *D,* Premature translocation of p47^{phox} to the cell membrane compartment in unstimulated Akita PMN. Cytoplasmic and membrane-associated proteins were extracted from unstimulated BM PMN and were size-fractionated on SDS-PAGE (80 μg protein/lane). Western blot shows p47^{phox} immunoreactivity exclusively in the cytoplasm in WT PMN, whereas in Akita PMN a portion of p47^{phox} is translocated to the cell membrane fraction. gp91^{phox} is found exclusively in the membrane fraction for both groups. The Western blot is representative of four separate experiments. A, Akita; Memb, membrane-associated protein extract; Cyt, cytoplasmic protein extract.

PMN migrated through the membrane of the Boyden chamber compared with WT PMN in response to fMLP (Fig. 1*A*). The chemotactic defect in Akita PMN was even more pronounced in response to the WKYMVm peptide (Fig. 1*B*).

Elevated superoxide release by isolated Akita PMN

Superoxide production was assessed in PMN isolated from WT and Akita peritoneal lavage fluid 12–14 h after zymosan A injection (29). Mean unstimulated baseline superoxide release was 45% higher in Akita mice (WT, 2.9 ± 2.0 nmol/min $\times 10^6$ cells; Akita: 4.3 ± 1.7 nmol/min $\times 10^6$ cells); however, this difference was not statistically significant ($p = 0.24$, $n = 6$ mice each group). Although fMLP induced superoxide release in both strains ($p < 0.01$), the increase in superoxide release in response to fMLP was significantly higher in Akita PMN compared with WT (Fig. 1*C*).

Acute glucose challenge does not alter PMN chemotaxis and superoxide release

To compare the effect of chronic hyperglycemia with short-term exposure to high glucose, isolated WT PMN were incubated in either 5.5 mM (normoglycemic) or 25 mM (hyperglycemic) medium for 3 h. Acute glucose challenge did not alter unstimulated random cell migration (WT PMN in 5.5 mM glucose, 3.6 ± 1.6 cells/mm^2; WT PMN in 25 mM glucose, 4.3 ± 0.8 cells/mm^2, $p = 0.45$, $n = 5$ mice each group). fMLP (10 nM) induced significant PMN chemotaxis in 5.5 mM ($p = 0.03$) as well as in 25 mM glucose ($p = 0.04$); however, the number of migrated cells were not different between the two groups (WT PMN in 5.5 mM glucose, 6.4 ± 1.6 cells/mm^2; WT PMN in 25 mM glucose, 7.7 ± 3.0 cells/mm^2, $p = 0.42$, $n = 5$ mice each group). Acute glucose challenge also failed to alter superoxide release at baseline (WT PMN in 5.5 mM glucose, 1.3 ± 0.7 nmol O^-_2/min $\times 10^6$ cells, WT PMN in 25 mM glucose, 1.5 ± 1.4 nmol O^-_2/min $\times 10^6$ cells, $p = 0.76$, $n = 6$ mice each group). fMLP (1 μM) elicited significant increase in superoxide release in both 5.5 mM ($p < 0.001$) and in 25 mM glucose ($p = 0.02$); however, stimulated superoxide release was similar in 5.5 and in 25 mM glucose (WT PMN in 5.5 mM glucose, 4.8 ± 0.7 nmol O^-_2/min $\times 10^6$ cells; WT PMN in 25 mM glucose, 3.6 ± 1.9 nmol O^-_2/min $\times 10^6$ cells, $p = 0.19$, $n = 6$ mice each group).

Partial translocation of p47^{phox} to the cell membrane fraction in unstimulated Akita PMN

To investigate hyperglycemia-induced alterations in the cellular machinery responsible for leukocyte superoxide release, unstimulated PMN from the BM pool were isolated and subcellular localization of p47^{phox} and gp91^{phox}, two key components of the NADPH oxidase were monitored with Western blotting. gp91^{phox}, a component of the membrane-bound flavocytochrome b_{558}, was found exclusively in the membrane fraction of both WT and Akita cell extracts. p47^{phox}, which resides exclusively in the cytoplasmic fraction of unstimulated WT PMN, was found partially translocated to the cell membrane in unstimulated Akita PMN, suggesting a primed or preactivated state in chronic hyperglycemia (Fig. 1*D*).

Enhanced alveolar bone loss in Akita mice after ligature-induced periodontal disease

Ligature-induced periodontal bone loss was used to assess the role of chronic hyperglycemia in the development of periodontal disease. A 9-0 silk ligature was tied around the left upper second molar, whereas the right upper second molar was left intact as a control. The silk ligature, similar to dental calculus, serves as a reservoir for oral bacteria and acts as a mechanical irritant as well, producing periodontal inflammation and bone loss (30). Ligation induced bone loss in both strains ($p < 0.01$; Fig. 2). However, the CEJ-ABC distance was significantly greater in Akita mice compared with similarly treated WT mice (Fig. 2). Bone loss in response to ligation as calculated by subtracting nonligated CEJ-ABC from corresponding ligated CEJ-ABC values were 0.092 ± 0.037 mm in WT and 0.157 ± 0.099 mm in Akita mice ($p = 0.02$, $n = 7$ mice each group).

Increased leukocyte rolling and attachment in Akita gingival microvessels

Rhodamine 6G-labeled leukocytes were monitored in gingival postcapillary venules in anesthetized WT and Akita mice using fluorescence microscopy to assess leukocyte-endothelium interactions in hyperglycemia in vivo. Unstimulated leukocytes of Akita mice displayed significantly enhanced rolling behavior during a 30-s observation period compared with WT cells ($p = 0.02$; Fig. 3). Intragingival injection of 100 ng TNF-α increased rolling cell numbers in both genotypes significantly ($p < 0.03$). However, no statistically significant difference was found between the two strains of mice in the increase in rolling cells attributable to TNF-α

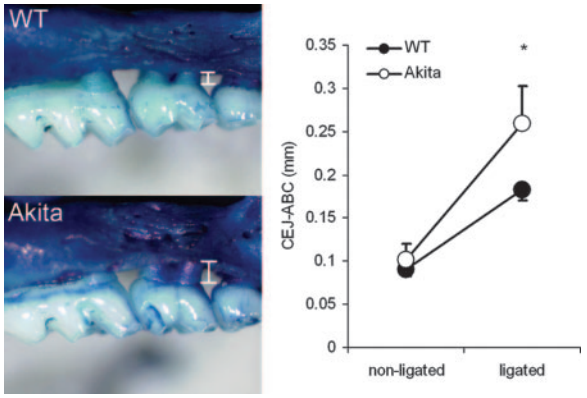

FIGURE 2. Alveolar bone loss following molar ligation in WT and Akita mice. Periodontal disease was induced by tying a silk ligature around the second maxillary molar (middle tooth) in WT (*top left*) and Akita (*bottom left*) mice for 3 wk. Alveolar bone loss was determined by measuring the distance between the CEJ-ABC (white bars). White, Enamel of the tooth crown; light blue, cementum of the exposed root surface; dark blue, alveolar bone of the maxilla. *Right panel,* Mean ± SD of CEJ-ABC measurements. On nonligated molars, there is no difference in the CEJ-ABC between WT and Akita mice. Ligation induces significantly more alveolar bone loss in Akita compared with WT mice ($p = 0.018$, $n = 7$ mice each group).

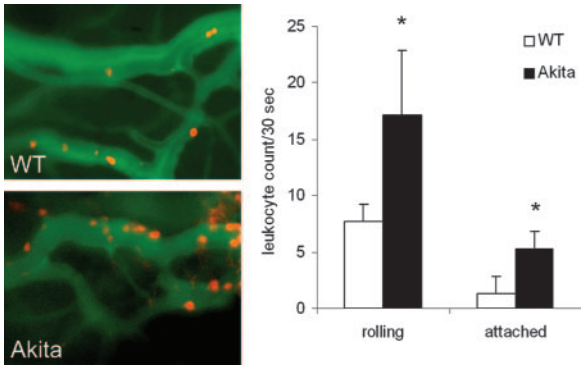

FIGURE 3. Intravital microscopy revealed elevated numbers of rolling and attached cells in gingival vessels of Akita mice. *Left panel,* Microscopic still images of rhodamine 6G-labeled leukocytes in the gingival microcirculation in unstimulated WT and Akita mice. Leukocytes rolling on or attached to the endothelium are visible in red; the microvasculature is labeled green using FITC-dextran. Original magnification, ×400. *Right panel,* The number of rolling and attached leukocytes in gingival venules (20–40 μm in diameter) during a 30-s observation period (rolling cells, $p = 0.016$ WT vs Akita; attached cells, $p = 0.032$ WT vs Akita, $n = 5$ mice each group).

(WT, 21 ± 4.9 leukocytes/30 s; Akita, 17.3 ± 7.5 leukocytes/30 s, $p = 0.47$, $n = 5$) or in the absolute number of rolling cells after TNF-α injection (WT, 28.8 ± 5.9 leukocytes/30 s; Akita, 33 ± 10.5 leukocytes/30 s, $p = 0.52$, $n = 5$). The number of attached cells was significantly higher in Akita mice compared with WT without stimulation ($p = 0.03$; Fig. 3). The number of attached cells also increased in response to TNF-α in both strains, albeit not significantly. The increase in the number of attached cells attributable to TNF-α stimulation was not significantly different (WT, 3 ± 1.4 leukocytes/30 s; Akita, 2 ± 1.4 leukocytes/30 s, $p = 0.59$, $n = 5$ mice each group). The absolute number of attached leukocytes after TNF-α was higher in Akita mice, although the difference did not reach statistical significance (WT, 3.3 ± 3.6 leukocytes/30 s; Akita, 6.5 ± 2.1 leukocytes/30 s, $p = 0.32$, $n = 5$ mice each group).

Discussion

Our findings indicate that chronic hyperglycemia primes the innate immune system for an exaggerated inflammatory response, including marked enhancements in cytokine and chemokine release, increased leukocyte marginalization, and exaggerated superoxide release. Chronic hyperglycemia also impairs PMN chemotaxis and augments ligature-induced periodontal bone loss. These findings expose significant changes in the innate immune response under chronic hyperglycemia, which may contribute to the development of periodontal disease and to other infectious lesions in diabetes as well. Among the classical proinflammatory cytokines, we have found IL-6 to be significantly more elevated in Akita compared with WT mice. TNF-α was only marginally affected and IL-1β response was indifferent to glycemic status. A similar cytokine pattern has been observed in humans, as plasma IL-6 levels are found consistently elevated in diabetic patients (31, 32), whereas increased TNF-α levels were reported only after acute glucose challenge (33, 34). In addition, we have identified three chemokines that are also profoundly affected by hyperglycemia, implying a broader range of effects of diabetes on leukocyte behavior than previously thought. Enhanced secretion of KC, a mouse analog of IL-8, indicates that chemotactic signaling to PMN and T cells is facilitated in hyperglycemia (35). MCP-1 secretion is similarly enhanced, targeting the chemotaxis of monocytes and T cells as well as basophils (36). The greatest increase, >4-fold in Akita lavage fluid compared with WT is in MIP-1α, a chemokine attracting T cells, monocytes/macrophages, and PMN (37). Defective MCP-1 down-regulation in the resolution phase of acute inflammation has been described in another diabetic model, the *db/db* mouse, where levels of MCP-1 along with TNF-α and MIP-2 remained high after bacterial infection, accompanied by a delay in the resolution of inflammation (38). Our data indicate that hyperglycemia not only can delay the decline of cytokines in the resolution phase but it will markedly augment the initial rise of a broad range of cytokines. Interestingly, elevated chemokine levels in abdominal lavage fluid 2 h after zymosan injection are followed by not higher but significantly lower leukocyte yields 12 h later, indicating an impaired leukocyte response to a broad range of chemokines in chronic hyperglycemia.

To assess the state of the inflammatory response under such an altered cytokine milieu, we studied the behavior of PMN. PMN function is essential for maintaining a healthy periodontium, as PMN deficiency in acute or chronic neutropenia results in gingivitis and oral ulcers (17). Congenital neutropenia (Kostmann disease) presents with persistent periodontal disease along with other severe infections (18). In Akita mice, we found decreased PMN chemotaxis in response to fMLP and to WKYMVm, a high-affinity ligand to the mouse formyl peptide receptor (39). Periodontal health is maintained as a balance between the immune defense and a diverse oral bacterial flora, and defects in PMN chemotaxis can lead to periodontal damage as it is demonstrated in localized aggressive periodontitis, a juvenile form of rapidly progressing periodontal disease (40).

Leukocyte rolling and attachment is increased in Akita gingival microvessels, indicating that the initial steps of leukocyte recruitment are enhanced in hyperglycemia. Leukocyte attachment is mediated by ICAM expressed on the endothelial and leukocyte cell surfaces, and increased expression of ICAM-1 was shown to contribute to leukocyte stasis in the diabetic retina (41). Our experiments demonstrate that intravital microscopy can be applied to gingival vessels in the mouse and show that chronic hyperglycemia without any further stimulation enhances leukocyte attachment to the gingival vessel wall. Taken together with the decreased

chemotactic migration of PMN, the enhanced marginalization in hyperglycemia may lead to leukocyte stasis along the vessel wall similar to the retinal microcirculation where leukocyte stasis is suspected to contribute to disease progression (41).

Although defective in chemotaxis, PMN appear to be partially activated by hyperglycemia as demonstrated by partial $p47^{phox}$ translocation and enhanced superoxide release. NADPH oxidase is the primary source of superoxide production in PMN (42). Components of the NADPH oxidase are dissociated in the resting state into cytoplasmic ($p47^{phox}$, $p67^{phox}$, and rac) and membrane-bound ($gp91^{phox}$ and $p22^{phox}$) components. Phosphorylation of $p47^{phox}$ and its translocation to the cell membrane is a key early event leading to full assembly of the NADPH oxidase and consequent production of superoxide (42). In BM-derived Akita PMN, a portion of $p47^{phox}$ molecules is membrane associated, indicating partial premature assembly of the NADPH oxidase in hyperglycemia. These effects of high blood glucose are similar to those observed after bacterial LPS stimulation. LPS by itself does not induce superoxide release but it facilitates $p47^{phox}$ translocation to the cell membrane, and superoxide release is increased after consequent fMLP stimulation, a phenomenon described as priming (43).

Oxidative stress has received considerable attention in the pathogenesis of diabetic complications as well as in the pathogenesis of diabetes itself. Glucose overload increases the mitochondrial transmembrane potential, resulting in elevated superoxide production (3). This has been suspected to contribute to cell damage in β cells and in endothelial cells, two cell types that are central to the pathogenesis and to the long-term complications of diabetes, respectively (44). In the case of infectious diseases, such as periodontal disease, superoxide production by leukocytes that are attached to the endothelium but fail to transmigrate may compound elevated superoxide levels already present in diabetic endothelial cells (3), thus further exacerbating oxidative stress on the microvasculature.

Although PMN are protective to the host under most circumstances, in several conditions PMN fail to differentiate between pathogen and host, resulting in tissue damage (19, 20). Direct tissue toxicity by PMN is mediated by superoxide, NO, and proteases (20). Indirectly, PMN contribute to inflammation and periodontal bone resorption by releasing TNF and IL-1 (45). In the periodontium, epithelial cells (46) and fibroblasts (47) are sensitive to PMN-mediated damage. Excessive superoxide release by PMN has been linked to periodontal disease in localized aggressive periodontitis (40, 48) and in diabetes (14, 49). Thus, it is conceivable that hyperglycemia delivers a double blow to periodontal health by preventing the transmigration of PMN to infected tissues and impairing proper antimicrobial defense, and also by increasing free radical load on the diabetic microvasculature.

Acute hyperglycemia applied to isolated WT PMN did not reproduce the leukocyte abnormalities observed in Akita mice. This observation supports the notion that the effects of chronic hyperglycemia on altered leukocyte behavior might be mediated by systemic factors such as circulating cytokines. Also, long-term exposure to high blood glucose might be necessary to change leukocyte function, a mechanism that might include the accumulation of advanced end-glycation products (15).

In addition to PMN, several other cell types are influenced by chronic hyperglycemia and may contribute to periodontal damage. Changes in endothelial cell function in response to hyperglycemia are perhaps the best characterized, including increased permeability, decreased NO release, and capillary occlusion (3). Endothelial dysfunction can directly lead to tissue damage by causing tissue ischemia. Alternatively, activated endothelial cells may activate leukocytes directly by expression of cell adhesion molecules, such as selectins, VCAM, and ICAM, or by expressing cytokines such as MCP-1 (36). Interestingly, adipocytes are also a significant source of proinflammatory cytokines, and inflammation is suspected to mediate obesity-induced diabetes (50). Conversely, the augmented cytokine response observed in hyperglycemia is likely to have broad effects in addition to regulating PMN function. Cytokine effects on bone metabolism are of particular interest in periodontal disease. For example, exaggerated IL-6 response in Akita mice may directly contribute to osteoclast activation and alveolar bone loss (45). Similarly MIP-1α, the chemokine most enhanced in Akita mice, potently enhances osteoclast formation (51), thus raising the possibility that MIP-1α directly enhances alveolar bone loss in Akita mice. The Akita cytokine pattern is also consistent with increased T cell recruitment, and receptor activator NF-κB ligand-mediated activation of osteoclast precursors by T cells has been shown to contribute to alveolar bone loss (16).

In summary, these findings indicate that inflammation in hyperglycemic milieu results in enhanced release of several cytokines, and the resulting changes in the innate immune system can contribute to secondary diabetic complications. In the periodontium, leukocyte defects induced by hyperglycemia may contribute to periodontal tissue damage by weakening the innate immune response to periodontal pathogens as well as by increasing free radical load on the gingival microvasculature.

Acknowledgments

We express gratitude for the expert help of Khadija Rhourida, Martha Warbington, and Jennifer Deady.

Disclosures

The authors have no financial conflict of interest.

References

1. Hogan, P., T. Dall, and P. Nikolov. 2003. Economic costs of diabetes in the US in 2002. *Diabetes Care* 26: 917–932.
2. Ceriello, A., and E. Motz. 2004. Is oxidative stress the pathogenic mechanism underlying insulin resistance, diabetes, and cardiovascular disease? The common soil hypothesis revisited. *Arterioscler. Thromb. Vasc. Biol.* 24: 816–823.
3. Brownlee, M. 2001. Biochemistry and molecular cell biology of diabetic complications. *Nature* 414: 813–820.
4. Nishikawa, T., D. Edelstein, X. L. Du, S. Yamagishi, T. Matsumura, Y. Kaneda, M. A. Yorek, D. Beebe, P. J. Oates, H. P. Hammes, et al. 2000. Normalizing mitochondrial superoxide production blocks three pathways of hyperglycaemic damage. *Nature* 404: 787–790.
5. van den Berghe, G., P. Wouters, F. Weekers, C. Verwaest, F. Bruyninckx, M. Schetz, D. Vlasselaers, P. Ferdinande, P. Lauwers, and R. Bouillon. 2001. Intensive insulin therapy in the critically ill patients. *N. Engl. J. Med.* 345: 1359–1367.
6. Dandona, P., P. Mohanty, A. Chaudhuri, R. Garg, and A. Aljada. 2005. Insulin infusion in acute illness. *J. Clin. Invest.* 115: 2069–2072.
7. Fogelstrand, L., J. Hulthe, L. M. Hulten, O. Wiklund, and B. Fagerberg. 2004. Monocytic expression of CD14 and CD18, circulating adhesion molecules and inflammatory markers in women with diabetes mellitus and impaired glucose tolerance. *Diabetologia* 47: 1948–1952.
8. Mohanty, P., W. Hamouda, R. Garg, A. Aljada, H. Ghanim, and P. Dandona. 2000. Glucose challenge stimulates reactive oxygen species (ROS) generation by leucocytes. *J. Clin. Endocrinol. Metab.* 85: 2970–2973.
9. Lin, Y., A. H. Berg, P. Iyengar, T. K. Lam, A. Giacca, T. P. Combs, M. W. Rajala, X. Du, B. Rollman, W. Li, M. Hawkins, et al. 2005. The hyperglycemia-induced inflammatory response in adipocytes: the role of reactive oxygen species. *J. Biol. Chem.* 280: 4617–4626.
10. Aljada, A., H. Ghanim, P. Mohanty, T. Syed, A. Bandyopadhyay, and P. Dandona. 2004. Glucose intake induces an increase in activator protein 1 and early growth response 1 binding activities, in the expression of tissue factor and matrix metalloproteinase in mononuclear cells, and in plasma tissue factor and matrix metalloproteinase concentrations. *Am. J. Clin. Nutr.* 80: 51–57.
11. Hansen, T. K., S. Thiel, P. J. Wouters, J. S. Christiansen, and G. Van den Berghe. 2003. Intensive insulin therapy exerts antiinflammatory effects in critically ill patients and counteracts the adverse effect of low mannose-binding lectin levels. *J. Clin. Endocrinol. Metab.* 88: 1082–1088.
12. Langouche, L., I. Vanhorebeek, D. Vlasselaers, S. Vander Perre, P. J. Wouters, K. Skogstrand, T. K. Hansen, and G. Van den Berghe. 2005. Intensive insulin therapy protects the endothelium of critically ill patients. *J. Clin. Invest.* 115: 2277–2286.
13. Grossi, S. G., and R. J. Genco. 1998. Periodontal disease and diabetes mellitus: a two-way relationship. *Ann. Periodontol.* 3: 51–61.

14. Karima, M., A. Kantarci, T. Ohira, H. Hasturk, V. L. Jones, B. H. Nam, A. Malabanan, P. C. Trackman, J. A. Badwey, and T. E. Van Dyke. 2005. Enhanced superoxide release and elevated protein kinase C activity in neutrophils from diabetic patients: association with periodontitis. *J. Leukocyte Biol.* 78: 862–870.
15. Lalla, E., I. B. Lamster, M. Feit, L. Huang, A. Spessot, W. Qu, T. Kislinger, Y. Lu, D. M. Stern, and A. M. Schmidt. 2000. Blockade of RAGE suppresses periodontitis-associated bone loss in diabetic mice. *J. Clin. Invest.* 105: 1117–1124.
16. Mahamed, D. A., A. Marleau, M. Alnaeeli, B. Singh, X. Zhang, J. M. Penninger, and Y. T. Teng. 2005. G^- anaerobes-reactive $CD4^+$ T-cells trigger RANKL-mediated enhanced alveolar bone loss in diabetic NOD mice. *Diabetes* 54: 1477–1486.
17. Boxer, L. A., R. Hutchinson, and S. Emerson. 1992. Recombinant human granulocyte-colony-stimulating factor in the treatment of patients with neutropenia. *Clin. Immunol. Immunopathol.* 62: S39–S46.
18. Carlsson, G., and A. Fasth. 2001. Infantile genetic agranulocytosis, morbus Kostmann: presentation of six cases from the original "Kostmann family" and a review. *Acta Paediatr.* 90: 757–764.
19. Weiss, S. J. 1989. Tissue destruction by neutrophils. *N. Engl. J. Med.* 320: 365–376.
20. Witko-Sarsat, V., P. Rieu, B. Descamps-Latscha, P. Lesavre, and L. Halbwachs-Mecarelli. 2000. Neutrophils: molecules, functions and pathophysiological aspects. *Lab. Invest.* 80: 617–653.
21. Serhan, C. N., A. Jain, S. Marleau, C. Clish, A. Kantarci, B. Behbehani, S. P. Colgan, G. L. Stahl, A. Merched, N. A. Petasis, et al. 2003. Reduced inflammation and tissue damage in transgenic rabbits overexpressing 15-lipoxygenase and endogenous anti-inflammatory lipid mediators. *J. Immunol.* 171: 6856–6865.
22. Yoshioka, M., T. Kayo, T. Ikeda, and A. Koizumi. 1997. A novel locus, Mody4, distal to D7Mit189 on chromosome 7 determines early-onset NIDDM in nonobese C57BL/6 (Akita) mutant mice. *Diabetes* 46: 887–894.
23. Wang, J., T. Takeuchi, S. Tanaka, S. K. Kubo, T. Kayo, D. Lu, K. Takata, A. Koizumi, and T. Izumi. 1999. A mutation in the insulin 2 gene induces diabetes with severe pancreatic β-cell dysfunction in the Mody mouse. *J. Clin. Invest.* 103: 27–37.
24. Izumi, T., H. Yokota-Hashimoto, S. Zhao, J. Wang, P. A. Halban, and T. Takeuchi. 2003. Dominant negative pathogenesis by mutant proinsulin in the Akita diabetic mouse. *Diabetes* 52: 409–416.
25. Haseyama, T., T. Fujita, F. Hirasawa, M. Tsukada, H. Wakui, A. Komatsuda, H. Ohtani, A. B. Miura, H. Imai, and A. Koizumi. 2002. Complications of IgA nephropathy in a non-insulin-dependent diabetes model, the Akita mouse. *Tohoku J. Exp. Med.* 198: 233–244.
26. Ueno, Y., F. Horio, K. Uchida, M. Naito, H. Nomura, Y. Kato, T. Tsuda, S. Toyokuni, and T. Osawa. 2002. Increase in oxidative stress in kidneys of diabetic Akita mice. *Biosci. Biotechnol. Biochem.* 66: 869–872.
27. Veihelmann, A., A. Hofbauer, F. Krombach, M. Dorger, M. Maier, H. J. Refior, and K. Messmer. 2002. Differential function of nitric oxide in murine antigen-induced arthritis. *Rheumatology* 41: 509–517.
28. Gyurko, R., H. Shoji, R. A. Battaglino, G. Boustany, F. C. Gibson III, C. A. Genco, P. Stashenko, and T. E. Van Dyke. 2005. Inducible nitric oxide synthase mediates bone development and *P. gingivalis*-induced alveolar bone loss. *Bone* 36: 472–479.
29. Bannenberg, G. L., N. Chiang, A. Ariel, M. Arita, E. Tjonahen, K. H. Gotlinger, S. Hong, and C. N. Serhan. 2005. Molecular circuits of resolution: formation and actions of resolvins and protectins. *J. Immunol.* 174: 4345–4355.
30. Lohinai, Z., J. G. Mabley, E. Feher, A. Marton, K. Komjati, and C. Szabo. 2003. Role of the activation of the nuclear enzyme poly(ADP-ribose) polymerase in the pathogenesis of periodontitis. *J. Dent. Res.* 82: 987–992.
31. Yu, W. K., W. Q. Li, N. Li, and J. S. Li. 2003. Influence of acute hyperglycemia in human sepsis on inflammatory cytokine and counterregulatory hormone concentrations. *World J. Gastroenterol.* 9: 1824–1827.
32. Esposito, K., F. Nappo, R. Marfella, G. Giugliano, F. Giugliano, M. Ciotola, L. Quagliaro, A. Ceriello, and D. Giugliano. 2002. Inflammatory cytokine concentrations are acutely increased by hyperglycemia in humans: role of oxidative stress. *Circulation* 106: 2067–2072.
33. Muller, S., S. Martin, W. Koenig, P. Hanifi-Moghaddam, W. Rathmann, B. Haastert, G. Giani, T. Illig, B. Thorand, and H. Kolb. 2002. Impaired glucose tolerance is associated with increased serum concentrations of interleukin 6 and co-regulated acute-phase proteins but not TNF-α or its receptors. *Diabetologia* 45: 805–812.
34. Spranger, J., A. Kroke, M. Mohlig, K. Hoffmann, M. M. Bergmann, M. Ristow, H. Boeing, and A. F. Pfeiffer. 2003. Inflammatory cytokines and the risk to develop type 2 diabetes: results of the prospective population-based European Prospective Investigation into Cancer and Nutrition (EPIC)-Potsdam study. *Diabetes* 52: 812–817.
35. Chen, L. Y., J. J. Shieh, B. Lin, C. J. Pan, J. L. Gao, P. M. Murphy, T. F. Roe, S. Moses, J. M. Ward, E. J. Lee, et al. 2003. Impaired glucose homeostasis, neutrophil trafficking and function in mice lacking the glucose-6-phosphate transporter. *Hum. Mol. Genet.* 12: 2547–2558.
36. Charo, I. F., and M. B. Taubman. 2004. Chemokines in the pathogenesis of vascular disease. *Circ. Res.* 95: 858–866.
37. Maurer, M., and E. von Stebut. 2004. Macrophage inflammatory protein-1. *Int. J. Biochem. Cell Biol.* 36: 1882–1886.
38. Naguib, G., H. Al-Mashat, T. Desta, and D. T. Graves. 2004. Diabetes prolongs the inflammatory response to a bacterial stimulus through cytokine dysregulation. *J. Invest. Dermatol.* 123: 87–92.
39. He, R., L. Tan, D. D. Browning, J. M. Wang, and R. D. Ye. 2000. The synthetic peptide Trp-Lys-Tyr-Met-Val-D-Met is a potent chemotactic agonist for mouse formyl peptide receptor. *J. Immunol.* 165: 4598–4605.
40. Van Dyke, T. E., and J. Vaikuntam. 1994. Neutrophil function and dysfunction in periodontal disease. *Curr. Opin. Periodontol.* 2: 19–27.
41. Miyamoto, K., S. Khosrof, S. E. Bursell, R. Rohan, T. Murata, A. C. Clermont, L. P. Aiello, Y. Ogura, and A. P. Adamis. 1999. Prevention of leukostasis and vascular leakage in streptozotocin-induced diabetic retinopathy via intercellular adhesion molecule-1 inhibition. *Proc. Natl. Acad. Sci. USA* 96: 10836–10841.
42. Robinson, J. M., T. Ohira, and J. A. Badwey. 2004. Regulation of the NADPH-oxidase complex of phagocytic leukocytes: recent insights from structural biology, molecular genetics, and microscopy. *Histochem. Cell Biol.* 122: 293–304.
43. DeLeo, F. R., J. Renee, S. McCormick, M. Nakamura, M. Apicella, J. P. Weiss, and W. M. Nauseef. 1998. Neutrophils exposed to bacterial lipopolysaccharide upregulate NADPH oxidase assembly. *J. Clin. Invest.* 101: 455–463.
44. Wiernsperger, N. F. 2003. Oxidative stress as a therapeutic target in diabetes: revisiting the controversy. *Diabetes Metab.* 29: 579–585.
45. Baker, P. J. 2000. The role of immune responses in bone loss during periodontal disease. *Microbes Infect.* 2: 1181–1192.
46. Altman, L. C., C. Baker, P. Fleckman, D. Luchtel, and D. Oda. 1992. Neutrophil-mediated damage to human gingival epithelial cells. *J. Periodontal Res.* 27: 70–79.
47. Deguchi, S., T. Hori, H. Creamer, and W. Gabler. 1990. Neutrophil-mediated damage to human periodontal ligament-derived fibroblasts: role of lipopolysaccharide. *J. Periodontal Res.* 25: 293–299.
48. Shapira, L., B. Gordon, M. Warbington, and T. E. Van Dyke. 1994. Priming effect of *Porphyromonas gingivalis* lipopolysaccharide on superoxide production by neutrophils from healthy and rapidly progressive periodontitis subjects. *J. Periodontol.* 65: 129–133.
49. Cutler, C. W., P. Eke, R. R. Arnold, and T. E. Van Dyke. 1991. Defective neutrophil function in an insulin-dependent diabetes mellitus patients: a case report. *J. Periodontol.* 62: 394–401.
50. Lazar, M. A. 2005. How obesity causes diabetes: not a tall tale. *Science* 307: 373–375.
51. Yu, X., Y. Huang, P. Collin-Osdoby, and P. Osdoby. 2004. CCR1 chemokines promote the chemotactic recruitment, RANKL development, and motility of osteoclasts and are induced by inflammatory cytokines in osteoblasts. *J. Bone Miner. Res.* 19: 2065–2077.